

# FRACTAL CHARACTERISATION OF CONCRETE DAMAGE IN THE STRAIN-SOFTENING REGIME

Alberto CARPINTERI and Stefano INVERNIZZI

*Department of Structural Engineering and Geotechnics,  
Politecnico di Torino, Corso Duca degli Abruzzi 24, 10129 Torino, Italy*

## ABSTRACT

In a previous work the authors showed how to acquire the meso-structural characteristics of undamaged concrete-like materials by a peculiar laser equipment. In order to extend the analysis to damaged disordered materials, a new direct tension test equipment has been developed, that minimizes flexural effects by freely rotating boundary conditions. Increasing levels of damage are obtained, after reaching the peak load, by proceeding along the descending strain-softening curve. After the desired damage level is reached, the load is removed and the specimen is cut to permit the laser acquisition of the most damaged zone. The progressive rarefaction of the effective stress-carrying cross section is described by means of fractal concepts. It is worth noting that both the fractal dimension and the measure of the stress carrying cross section decrease after the peak load, and vanish when the specimen is broken apart.

## INTRODUCTION

The disordered microstructure of concrete is responsible for the peculiar features of the fracture phenomenon. Stable crack growth, ductile-brittle transition and size effects are not explicable in the classical framework. Pre-existing pores, debonded zones and microcracks interact with each other in a complex manner. Attempts to describe such behaviour by means of deterministic micromechanics models are deemed to be incomplete or even misleading. Even the most sophisticated measurement of material properties, coupled with the use of most powerful computers, would not succeed in the exact (deterministic) modelization of the fracture phenomenon. The local aspects of cracks (e.g. position, shape, width, growth rate) are neither measurable nor predictable. On the contrary, the global aspects, e.g. the invariant features, can be put into evidence by approaching the problem from a completely new viewpoint. Cooperative phenomena are nowadays successfully interpreted by means of alternative methods, such as catastrophe theory, fractals, renormalization group theory and chaos dynamics. In particular, the combination of fractal geometry with renormalization provides new insights towards the understanding of concrete fracture [1]. Modelization of the microstructure by means of fractal domains permits to capture the hierarchical and self-organized aspect of damage accumulation and crack propagation. An essential aspect is in fact represented by the lacunarity of the porous microstructure, which represents a random field and explains the size effect on the nominal tensile strength.

In the present paper, dog-bone concrete specimens subjected to uniaxial tensile tests up to different damage levels are considered. The test-machine is provided with two spherical joints that allow the load to remain centered after the peak load is reached, i.e. during the softening regime. An innovative experimental methodology, developed at the Department of Structural Engineering and Geotechnics of

Table 1: COMPRESSION TESTS.

#	Size [cm]	Size [cm]	Section Area [cm <sup>2</sup> ]	Peak Load [daN]	Compression Strength [daN/cm <sup>2</sup> ]
1	16.0	16.0	256.0	94300	368
2	16.2	16.2	262.4	101300	386
3	16.1	16.0	257.6	94100	365
4	16.2	16.0	259.2	100900	389
MEAN					377

Table 2: RILEM THREE POINT BENDING TESTS.

#	Weight kg	Length [mm]	Height [mm]	Depth [mm]	Span [mm]	Notch Length [mm]	Fracture Energy $\mathcal{G}_F$ [N/m]
1	23.880	1000	100	100	800	49.5	137.1
2	24.040	1000	100	100	800	49.5	82.9
3	24.265	1000	100	100	800	51.0	96.3
4	23.690	1000	100	100	800	50.0	83.5
MEAN							100.0

the Politecnico di Torino, has been used to analyze the microstructural characteristics of the progressively damaged concrete. By means of a completely automatized laser system, the 3D morphologies of concrete can be digitized. This procedure, which yields the effective depth and shape of the pores, permits to overcome the drawbacks and ambiguities of traditional image analysis techniques, where dark particles often confuse with pores.

In previous papers, planar cross-sections of the virgin material were considered, and the pore and void distribution (like the moon-craters distribution) were easily extracted from the (detrended and filtered) laser-scanned topography. That investigation allowed the authors to confirm the lacunar fractal character of the ligament [2], as well as the self-similar character of the pore size distribution, which has been recently assumed in various statistical models of brittle fracture [3].

Now, the same procedure is applied to partially damaged specimens, at different load levels, in order to investigate on the progressive rarefaction of the resisting ligament.

As a result of the damage increase, not only the measure of the effective stress carrying cross section, but even its fractal dimension decreases.

## THE CONCRETE TENSION TEST

Although modern displacement servo-controlled closed loop test machines allow, in principle, to measure the load-displacement curve in the softening regime, concrete testing in tension is particularly difficult. In fact, due to the propagation of cracks after the reaching of the peak load the actual section loses its symmetry with respect to the applied load, and disturbing flexural effects arise. In order to avoid such effects completely, three orthogonal actuators can be used to perform uniform displacement tests [4]. Otherwise, it is possible to minimize flexural effects if particular care is taken to the load boundary conditions. If the loading platens are both freely rotating, the load is automatically re-centered (at least to a certain amount) as soon as the section geometry varies due to fracture enucleation. While other authors performed similar tests on notched specimens [5], in the present work un-notched dog-bone shaped concrete specimens are considered.

Normal portland concrete has been used for casting eighteen dog-bone specimens. Prior to the tensile tests, the material has been characterized from a mechanical point of view, performing standardized compression tests on cube (see Table 1) and RILEM three point bending tests [6] (see Table 2). The mean compression strength is equal to  $377 \text{ daN/cm}^2$ , while the mean fracture energy is  $100 \text{ N/m}$ .

The complete mechanical characterization of the testing material is indispensable to a correct design of the displacement measurement bases ( $68 \text{ mm}$  in our case), in order to avoid snap back behaviours. The

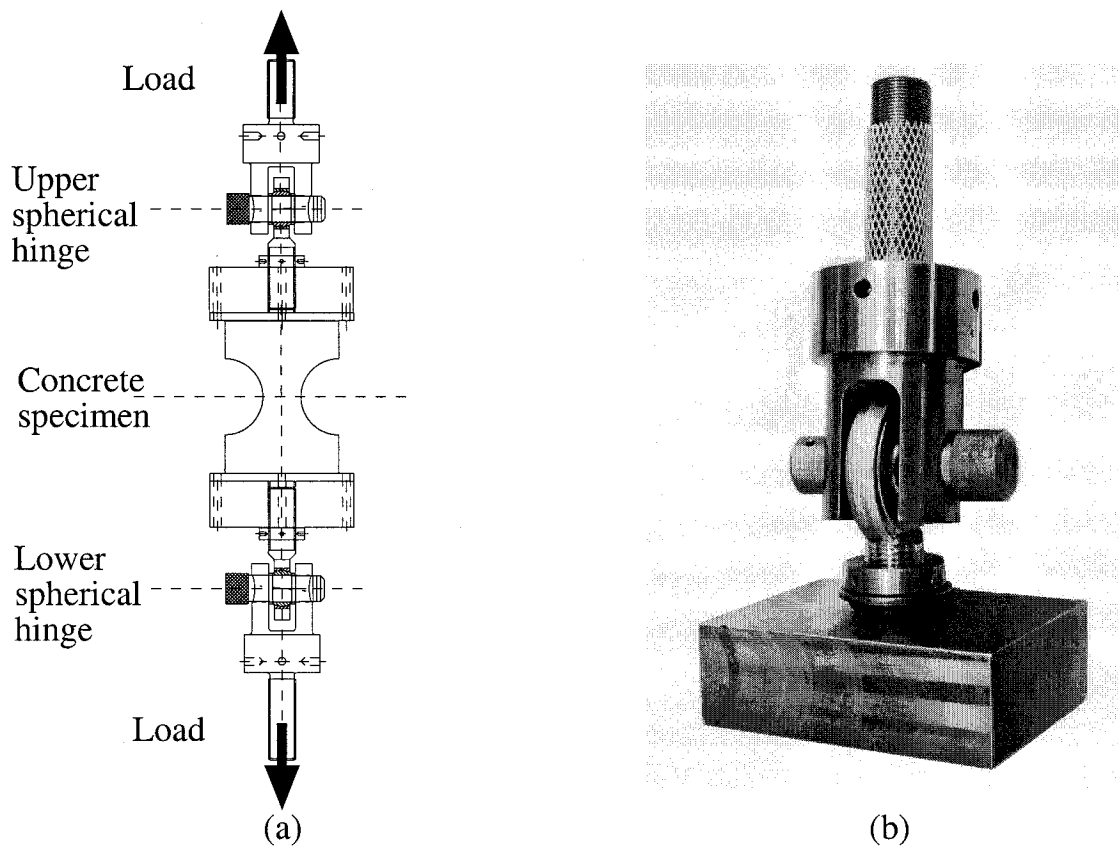


Figure 1: Diagram of the apparatus (a). Upper spherical hinge and rigid platen (b).

test apparatus scheme is shown in Figure 1a. The upper and the lower spherical hinges are realized with two SA 35 TE-2RS steel on teflon terminals (SKF<sup>TM</sup>). On one side, they are linked by a removable gudgeon to a crotch fixed to the MTS<sup>TM</sup> load actuator. On the other side, rigid thick platens are provided to connect the specimens. The concrete specimens (Figure 2a) are previously glued to two thin platens by using an epoxy two-component resin (Starcement 2XN by MPM<sup>TM</sup>), that allows easy positioning and removal from the test apparatus.

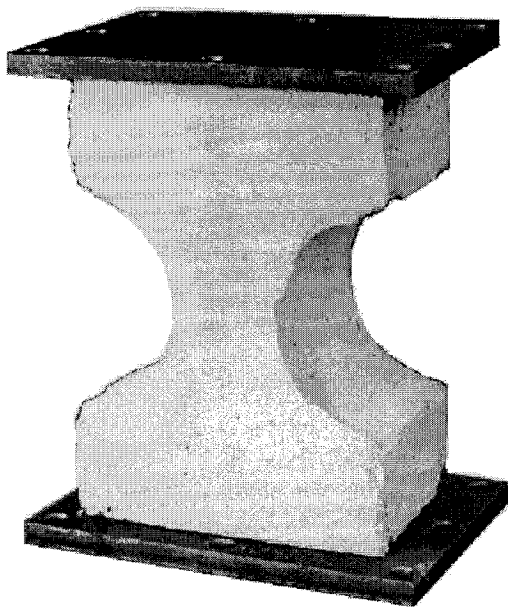
To perform the displacement controlled tests, the mean value of four measurement bases was considered as feedback. Each displacement was acquired by DD1 displacement transducers, two for each side of the specimen, placed around the thinner zone, where damage localization is more likely to occur (Figure 2b). This choice allows also to evaluate the magnitude of flexural effects during the softening regime. In Figure 3a, a load-displacement curve is shown, with respect to the mean elongation as well as for each displacement acquisition. It is worth noting that a very small compression can be appreciated, confirming the efficiency of the collinear hinges mechanism.

In order to study the damage evolution by means of fractal concepts, the true stress-carrying cross sections referring to different levels of damage are to be compared. Therefore, specimens are grouped and subjected to increasing deformations, after the peak load is reached. The damage control variable  $D$  is equal to:

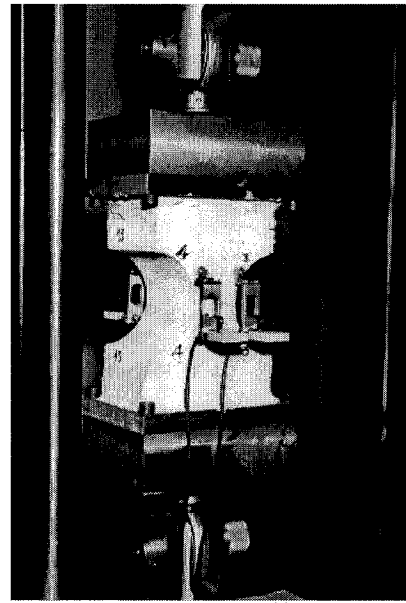
$$D = 1 - \frac{P_u}{P_p}, \quad (1)$$

where  $P_p$  is the peak load and  $P_u$  is the load reached just before unloading. In this way, damage is zero before the peak load, increases descending along the softening curve, and is equal to one when the specimen is completely broken apart. For each group, once a certain damage is accumulated in the specimen the load has been removed. Four levels of damage have been chosen, ranging from undamaged material (just after the peak load) to the complete separation of the specimen in two halves, as shown in Figure 3b.

The mean tension strength of the specimens is equal to  $1744 \text{ daN/mm}^2$ , with a standard deviation of  $178.6 \text{ daN/mm}^2$ . These results suggest that not a so dispersed value of tension strength is obtained



(a)



(b)

Figure 2: Dog-bone concrete specimen glued to the thin platens (a). View of the test equipment (b).

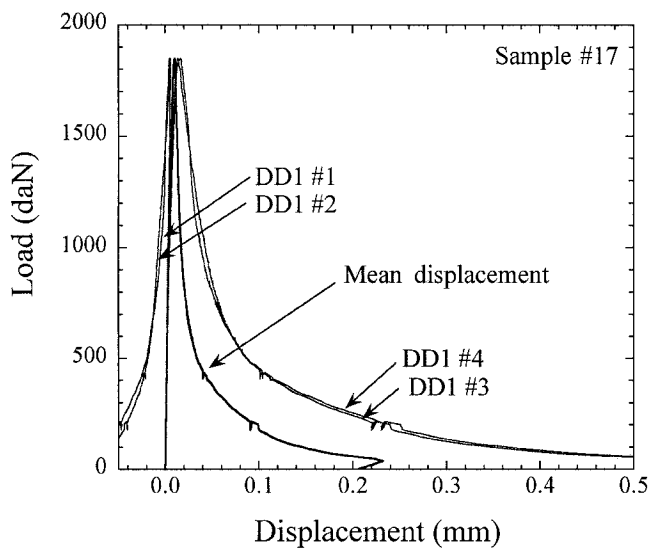
when the tests are carried out properly.

## THE LASER SCANNER ACQUISITION

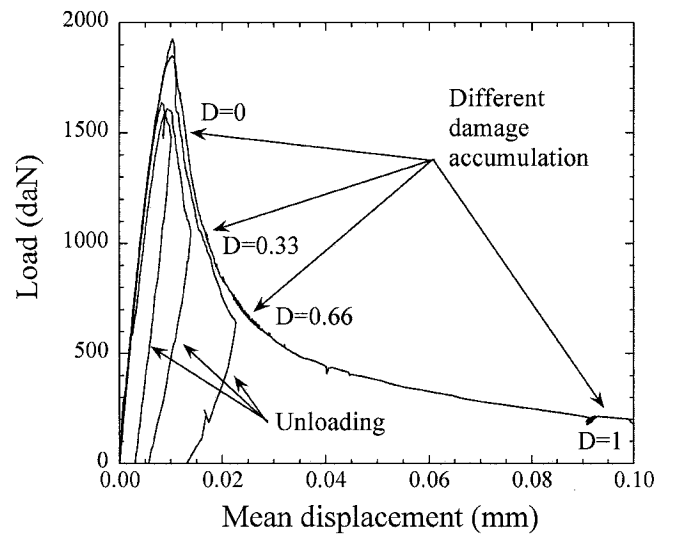
The main purpose of the experimental methodology, entirely developed at Politecnico di Torino [7], is to digitize the three-dimensional topography of surfaces at the meso-scale. The surface heights measurement is performed by means of a laser profilometer, by counting the number of wave-cycles between the ray emission and the ray reception after the reflection on the specimen surface. The specimen to be analyzed is rigidly framed into a solid truss, whereas the horizontal position of the distanziometer is controlled by two orthogonal micrometric step motors. The step motors interface and the data acquisition board that convert the analogical signal provided by the laser are both plugged in the same PC motherboard. A dedicated software provides extreme versatility and the full automation of the surface acquisition process. The digitized surfaces can extend over a  $50\text{mm} \times 100\text{mm}$  area, and a  $2\mu\text{m}$  maximum precision can be achieved, both in the vertical and horizontal directions.

In the study of the microstructural morphology of concrete it is useful to digitize planar cross sections obtained by cross-cutting progressively damaged specimens. These surfaces appear almost flat, with localized distribution of moon-like craters due to the intersection of the cutting plane with the inherent microstructural flaws. In Figure 4a, one cross-cutting surface is shown and compared with the numerical shaded-relief restitution of the acquired topography of Figure 4b. The presence of cavities is responsible for an effective resisting cross section that is less dense and compact than the nominal one. Furthermore, in real situations, the porosity is not uniform, and the relative percentage of voids depends on the linear size of the considered section.

The true stressed domain is made out of points not belonging to the craters, i.e. to the pore structure. Hence, from a theoretical point of view, the true resisting section can be evaluated by considering the set of points whose heights are exactly equal to the cutting plane height. Practically, the obtained surface is not absolutely plane and presents a low uniform roughness due to the cutting process that can be confused with the finer porosity. For this reason, another virtual plane has been considered, parallel to the cutting section, but at a lower height, which is able to intersect only the real cavities (Figure 5a). The points whose height is greater than the virtual plane height, are considered to belong to the real stress-carrying domain, while the remaining points belong to the (complementary) void set.



(a)



(b)

Figure 3: Load vs. displacement: four DD1 measurements and mean value (a). Different damage accumulation in the softening regime (b).

This procedure allows to filter out the noise produced by cutting. However, some information is lost about the finer porosity. To perform the virtual cut, it is also necessary to determine the mean real cutting plane by a detrending algorithm.

In Figure 5b, the theoretical evolution of the fractal dimension of the effective cross section is shown as a function of the virtual plane height, for increasingly damaged sections. When the virtual plane lays well beneath the real cutting plane, no voids are intersected; consequently, the calculated dimension is equal to 2 (Euclidean). Increasing the virtual plane height, more and more voids are intersected, and the fractal dimension decreases approaching a limit value that depends on the rarefaction (and thus on the damage) of the section. As soon as the virtual plane height exceeds the real cutting plane height, the dimension falls down to zero, since there are no more intersected points at all.

## THE FRACTAL ANALYSIS OF DAMAGED CROSS SECTIONS

The fractal dimension of the effective stress-carrying domain has been calculated by using two different algorithms.

Based on the concept of covering, the box-counting method estimates the fractal dimension as a function of the vanishing order of the covering area. The number of boxes  $N_i$ , needed to cover the set, is calculated for a decreasing value of the side  $d$  of the square covering element. The stress-carrying cross section is a self-similar lacunar fractal in a statistical sense. Then the following equation holds:

$$\Delta_{\text{box}} = \lim_{d \rightarrow 0} \frac{\log N_i}{\log (1/d)}. \quad (2)$$

The fractal dimension can be also evaluated by referring to the mass logarithmic density. If the effective cross section were characterized by a uniform distribution of cavities, it would be possible to calculate the density defined as the ratio of the effective area  $A_{\text{eff}}$  to the nominal area  $A_{\text{nom}}$ . In the actual case, this density can not be unambiguously calculated, because it depends on the resolution and on the size of the considered area. In fact, the complex distribution of the pores causes the probability of finding large cavities to be higher as the size of the considered area increases (like in a natural sponge [8]). The classical density is not constant, but decreases by increasing the nominal size. To obtain a scale-invariant value, it is necessary to refer to the logarithmic density, which is defined as:

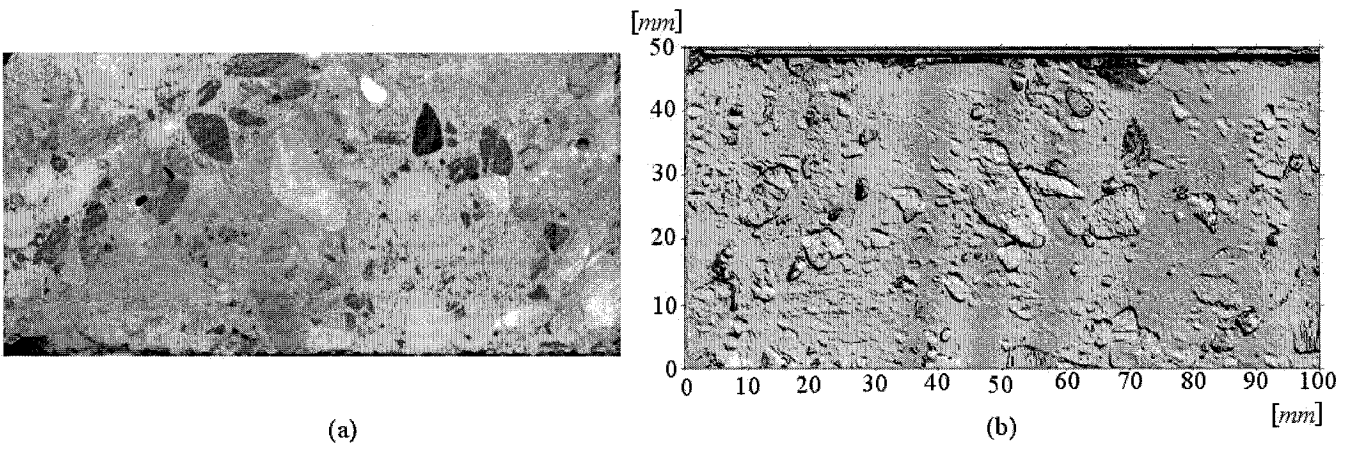


Figure 4: Traditional image analysis (a). Shaded relief restitution of the laser scanned surface (b).

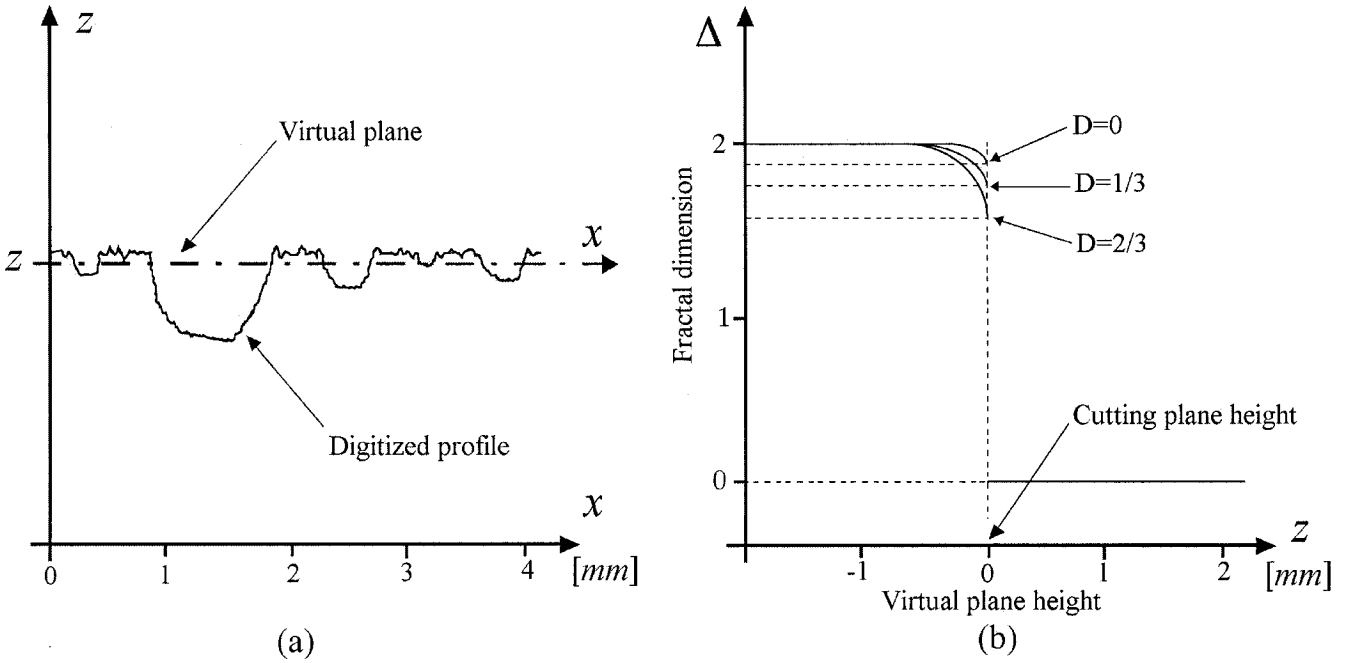


Figure 5: Scheme of the virtual section (a). Expected theoretical evolution of the fractal dimension for growing damage level (b).

$$\rho_{\log} = \frac{\log A_{\text{eff}}}{\log A_{\text{nom}}} \quad (3)$$

If  $d$  is the linear size of the considered area, the fractal dimension  $\Delta_{\log}$  can be evaluated as the limit slope of the bilogarithmic diagram  $\log A_{\text{eff}}$  versus  $\log d$ .

The fractal dimension calculation has been performed for each virtual plane position to obtain the curve of complete dimension evolution. Because of the cutting noise, the theoretical diagram of Figure 5b can not be recovered exactly. Therefore, the experimental curves of Figure 6 are characterized by a transition smoother than expected. Nevertheless, a general trend can be recognized, i.e. decreasing of the stress-carrying cross section fractal dimension for increasing damage levels. While the ligament measure decrease is due to macro fracture coalescence, the decrease of the fractal dimension is reasonably ascribed to the micro- and meso-fracture enucleation as well as to evolution in the inherent porosity. Although the general trend is rather unambiguously recognized, on the other hand the cutting noise does not permit a quantitative evaluation of fractal dimension  $\Delta$  vs. damage variable  $D$ .

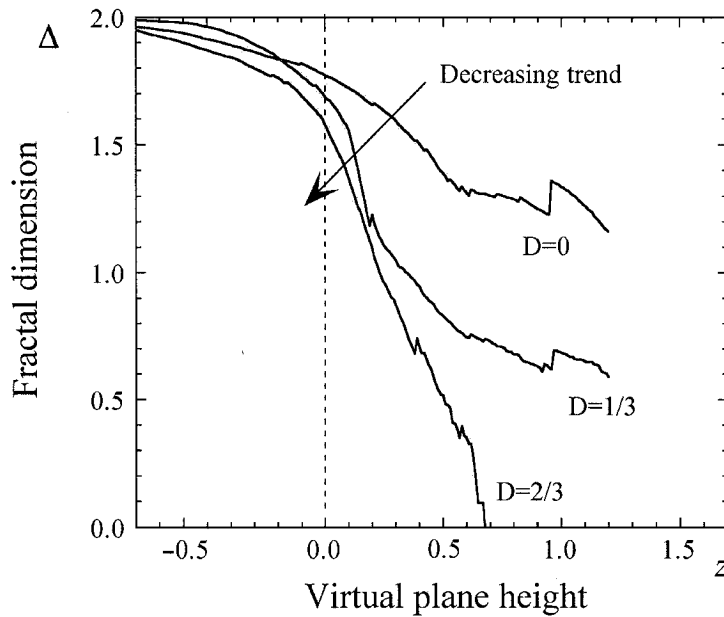


Figure 6: Experimental decrease of the stress-carrying cross section fractal dimension for increasing levels of damage.

## CONCLUSIONS

A new direct tension test equipment has been developed that minimizes flexural effects on concrete dog-bone shaped unnotched specimens. Progressively damaged specimens have been sawn and laser scanned in order to obtain the topography of the cut surface. This procedure allows to obtain the true stress-carrying domain. The damage evolution during the softening regime has been characterized by means of fractal geometry. The general decreasing trend of the ligament fractal dimension with respect to increasing damage can be recognized rather easily. This dimension lowering is probably due to micro- and meso-fracture enucleation as well as inherent porosity evolution, and has not to be confused with the classical measure decreasing, to be ascribed to macro-fracture propagation throughout the specimen. While the macro-fractures are detectable only at the final stage of the softening tail, the fracture nucleation (and then the dimension decreasing) seems to be a more progressive phenomenon. The main drawback appears to be the saw-cutting step. In order to obtain the quantitative  $\Delta$  vs.  $D$  relation between the ligament fractal dimension and the damage variable, an improvement of the present sawing technique is required.

## ACKNOWLEDGEMENTS

The present research was carried out with the financial support of the Ministry of University and Scientific Research (MURST), the National Research Council (CNR) and the EC-TMR Contract N° ERB-FMRXCT 960062. Thanks are also due to Mr. Vincenzo Di Vasto for carefully performing the testing programme.

## REFERENCES

- [1] Carpinteri, A. (1994). *Mechanics of Materials*, **18**, pp. 259-266.

- [2] Carpinteri, A., Chiaia, B. and Invernizzi, S. (1999). *Theoretical and Applied Fracture Mechanics*, **31**, pp. 163-172.
- [3] Carpinteri, A., Ferro, G. and Invernizzi, S. (1997). *Engineering Fracture Mechanics*, **58**, pp. 421-435.
- [4] Carpinteri, A., Ferro, G. (1994). *Materials and Structures (RILEM)*, **27**, pp. 563-571.
- [5] Van Mier, J.G.M., Schlangen, E. and Vervuurt, A. (1994). In *Fracture and Damage of Quasibrittle Structures*, pp. 289-301, Bažant, Z.P., et al. (Eds.), E&FN Spon, London/New York.
- [6] TC-50 FMC Draft Recommendation (1985). *Materials and Structures (RILEM)*, **18**, pp. 287-290.
- [7] Carpinteri, A., Chiaia, B. and Invernizzi, S., (1998). In *Proceedings of the Twelfth European Conference on Fracture ECF 12 - Fracture from Defects*, **III**, pp. 1557-1562, Brown, M.W., de los Rios, E.R. and Miller, K.J. (Eds.), Emas Publishing, London.
- [8] Mandelbrot, B.B. (1982). *The Fractal Geometry of Nature*, W.H. Freeman & Co., San Francisco.